Geochemistry of orthoamphibole-bearing Archean rocks, central Tobacco Root Mountains, southwestern Montana

William H. Peck
Department of Geology, Beloit College, Beloit WI 53511

INTRODUCTION

The Spuhler Peak Formation (SPF) of Guillmeister (1971) is located in the central Tobacco Root Mountains and extends from the Branham Lakes area northwest to Spuhler Peak, Guillmeister's type location. The SPF is made up of interbedded amphibolites and ortho-amphibolites, with minor amounts of sillimanite schist, quartzite, and meta-ultramafics. The nature of the contact of the SPF with the metamorphic packages structurally above and below it is not well understood. Additionally, the protolith of this package has not been well constrained, and is the focus of this study.

PREVIOUS WORK

Burger (1966), Guillmeister (1971) and O'Neil (1983) have conducted mapping studies of areas of the Spuhler Peak Formation. Vitaliano and Cordua's (1979) compilation map provides a detailed look at the regional geology of the area. Cummings and McCulloch (1992) performed a geochemical study of amphibolites and ultramafic rocks of the SPF in the area Branham Lakes. They suggest that the amphibolites are tectonically emplaced metamorphosed oceanic crust. This suggestion is consistent with the small amounts of ocean-floor metasediments in the area (sillimanite schist and quartzite), but does not address the protolith the orthoamphibole-bearing rocks.

ORIGIN OF CORDIERITE-ORTHOAMPHIBOLE ROCKS

The cordierite-orthoamphibole metamorphic assemblage has received a great deal of attention because the chemistry of these rocks is not easily comparable to modern igneous or sedimentary rocks. These rocks are calcium deficient, so orthoamphibole ($(Mg,Fe)_7Si_8O_{22}(OH)_2$) is a major component as opposed to hornblende ($(Ca,Na)_{2-3}(Mg,Si,Al)_5Si_6(Si,Al)_2O_{22}(OH)_2$). Proposed processes to produce these rocks include: metasomatic addition of Fe and Mg and depletion of Ca (or re-distribution of Fe, Mg, and Ca) during metamorphism, partial melting of pelitic rock (leaving a Mg-rich, Ca-poor residuum), or chemical alteration prior to metamorphism. This last category includes rocks that were influenced by Mg-rich evaporitic waters, sub-aerial weathering, deuteric alteration, and hydrothermal alteration. A good summary of the history of this debate is given by Robinson and others (1982).

PETROGRAPHY

Samples containing ortho-amphiboles were collected from the SPF. They contain the assemblage garnet-orthoamphibole-quartz-plagioclase, with varying amounts of cummingtonite, hornblende, and cordierite with minor sillimanite and apatite. The rocks are consistently of high amphibolite grade. Iridescence in the orthoamphiboles caused by anthophyllite exsolution in gedrite is common.

GEOCHEMISTRY

Rocks were selected for eventual geochemistry work, so "fresh" samples were collected. Because of this the sampling bias is towards fine-grained, non-permeable specimens. Geochemical data for 23 samples (Table 1) was obtained using Beloit College's inductively coupled argon plasma spectrometer (ICAP) for both major and trace elements.

The major element geochemistry of the orthoamphibole-bearing rocks is in the range of basalts except for CaO, which averages 3.5 weight percent. When plotted on the Jensen Cation Diagram (Jensen, 1976) the samples fall in the field of high-iron tholeiitic basalts (Figures 1 and 2). However, a plot on the trace element discrimination diagram of Pearce and Cann (1973) falls in the field of calc-alkali basalts (Figure 3). Incompatible element ratios diverge from chondrite ratios. Al_2O_3/TiO_2 is lower than the chondrite value of 20 (Figure 4). Ti/Zr, Ti/Y, Y/Zr, and Sc/Zr are all lower than chondrite values of 110, 209, .39, and 1.4. La and Ce are enriched compared to chondritic values (and Y). There is a complex correlation between Sr and Ca (Figure 5).

DISCUSSION

It has been noted by many workers (e.g. Humphris and Thompson, 1978a) that hydrothermal alteration of basalts causes depletion in CaO and SiO_2 and enrichment of MgO and H_2O. Such hydrothermally altered basalts have the bulk-chemistry to serve as the protolith of cordierite-anthophyllite rocks (Robinson and others, 1982) in

fault could produce the strong kyanite lineation, and account for crystals that have been pulled apart in the direction of their long axes.

At some time after its emplacement, the SPF was extensively folded by at least two phases of deformation. The first phase was characterized by isoclinal folds with axes plunging 35 to 45 degrees to the NE. In outcrop, these F1 folds cause local repeats in section, and are refolded by broad, open folds with steeply plunging, north trending axes (Fig. 3). The contact between the SPF and the ICMS and PMMMC appears to have been folded into a large, isoclinal synform during the F1 phase, as its fold axis aligns well with those of the outcrop scale F1s (Fig.4). Folding probably occurred synchronously with the second metamorphism and melting event. Melt pockets near the contact are concentrated in fold noses, while farther back melt is concentrated in small (1 to 2cm) shears parallel to foliation. In fold noses, mineral crystallization times span the range from pre- to post-folding.

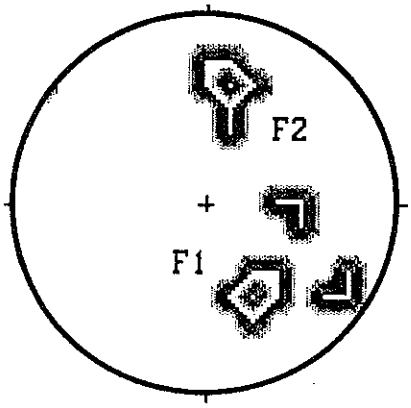

Fig. 3: Contoured equal area projection of poles to axial planes of folds in the SPF, showing two phases of folding.

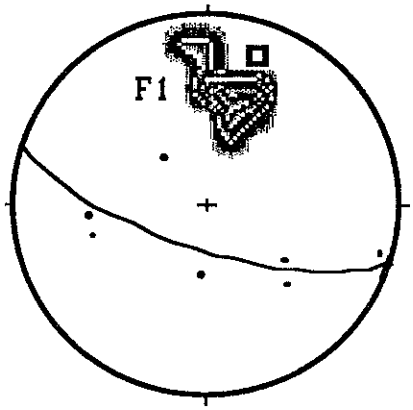

Fig. 4: Equal area projection of attitude of SPF contact (dots), fold axis of contact (box), and axes of F1 folds (contoured).

Conclusions: A Proposed Metamorphic and Deformational History

Given the field relationships, petrological and structural evidence, and conclusions of previous researchers, a sequence of events affecting the Spuhler Peak Formation in the Noble Lake area may be tentatively extrapolated to a partial history of the formation as a whole. Much of the following sequence is still open to interpretation and re-evaluation until geochemical data is available to test several apects of the present theory. Isotopic ages from within the SPF will help clarify some major timing questions. Since protoliths are as of yet unestablished, the history must begin with the first metamorphic event.

1) An upper amphibolite grade metamorphism formed the first amphibolites and quartzites, with the dominant assemblage; cpx-hbld-plag-gnt-qtz-biot. This event may have coincided with the 2.7 Ga event that affected the ICMS.

2) The SPF was emplaced above the ICMS and PMMMC along a thrust fault. Kyanite may have formed during the emplacement, but could also have been a component of the original metamorphic assemblages.

3) A second, lower pressure metamorphic event was accompanied by melting and folding. Sillimanite replaced kyanite, cordierite was formed, and pyroxene was hydrated to hornblende. The whole formation, including the contact, was folded into a large, isoclinal synform, with many parasitic isoclines along the limbs. Synchronous melting was concentrated close to the contact, as the fault chanelled fluids into the system to facilitate melting. This event may have been related to the high temperature event at 1.6 Ga recorded in nearby units. The second period of folding may have been continuous with the first, or may represent a seperate episode.

4) The final, low grade metamorphic event filled old fractures with chlorite and a new generation of biotite, possibly in the Cretaceous.

References Cited:

Burger, H. R., 1969, Structural evolution of the southwestern Tobacco Root Mountains, Montana: Geological Society of America Bulletin, v. 80, p. 1329-1342.

Friberg, N., 1976, Petrology of a metamorphic sequence of upper-amphibolite facies in the central Tobacco Root Mountains, southwestern Montana [Ph.D thesis]: Bloomington, Indiana, Indiana University, 146 p.

Gilletti, B. J., 1966, Isotopic ages from southwestern Montana: Journal of Geophysical Research, V. 71, p. 4029-4036.

Gillmeister, N. M., 1971, Petrology of Precambrian rocks in the central Tobacco Root Mountains, Madison County, Montana [Ph.D thesis]: Cambridge, Massachusetts, Harvard University, 210 p.

Mueller , P.A., and Cordua, W. S., 1976, Rb-Sr whole-rock ages of gneisses from the Horse Creek area, Tobacco Root Mountains, Montana: Isochron/West, v. 16, p. 33-36

most cases. It should be noted that some workers (e.g. Reinhardt, 1987) have recognized that muds affected by evaporite waters also have similar bulk compositions, but these rocks are usually have higher MgO than FeO.

The major element trend for these rocks correlates surprisingly well with a tholeiitic trend (Figures 1 and 2), especially when possible Mg enrichment is taken into account. The Jensen Cation Plot is used here instead of the AFM diagram (Irvine and Baragar, 1971) because it does not use Na_2O or K_2O (which are typically hydrothermally mobile) and distinguishes komatiitic rocks. The dividing line between tholeiitic and calc-alkalic fields "corresponds closely to those employed on the AFM diagram and the Al_2O_3 versus normative plagioclase composition diagram by Irvine and Baragar (1971)" (Jensen, 1976).

The use of "immobile" trace elements to determine the tectonomagmatic affinity of Archean rocks requires two major assumptions: 1) That trace element concentrations of rocks in the Archean were in the same ratios as the trace element concentrations for the "known" (modern) data set and 2) The "immobile" trace elements are truly immobile. I am not convinced that either of these conditions are satisfied. The SPF rocks have a definite calc-alkaline affinity on the Ti-Zr-Y discrimination plot of Pearce and Cann (1973) (Figure 3), but do not on the Jensen Cation Plot (Figure 2).

Ti, Zr, and Y are all transition metals, which have distribution coefficients that are highly sensitive to temperature. The higher geothermal gradient in the Archean would have lowered the distribution coefficient for Ti, Zr, and Y, which would enrich their concentrations in a magma produced by partial melting in the mantle. This would cause volcanic rocks to be enriched in incompatible elements. If the dependence on temperature for Ti, Zr, and Y are slightly different, then the higher geothermal gradient could cause relative enrichment and depletion between these elements, making the fields of Pearce and Cann (1973) valid only for modern mantle compositions and temperatures.

Ti, Zr, and Y are reported by many workers as "immobile" during hydrothermal alteration (e.g. Humphris and Thompson, 1978b). There are some cases, however, where this does not seem to be the case. MacGeehan and MacLean (1980) report hydrothermally altered sea-floor basalts that have been depleted in FeO, MgO, CaO, TiO_2, P_2O_5, and other trace metals while being enriched in SiO_2, Zr, Y, and REE. This alteration makes them appear to be evolved calc-alkaline rocks when they were originally MORBs. I do not think there has been any such "silicification" in the SPF rocks, but the immobility of the transition metals can not be assumed.

The SPF rocks appear to have undergone hydrothermal alteration. The correlation of Sr with Ca is common in hydrothermally altered basalts (Humphris and Thompson, 1978b), probably due to the dissolution some phase containing a constant Ca/Sr ratio. This Ca/Sr correlation is seen in the SPF rocks (Figure 5). Also plotted are two non-orthoamphibole bearing amphibolites from the SPF, showing that hydrothermal alteration was not restricted to the now orthoamphibole-bearing rocks. The two distinct linear trends could represent two original protoliths with different Ca/Sr ratios, or different hydrothermal events. There is no geographic constraint as to whether the rocks plot in the upper or lower trend, sometime rocks collected five meters apart fall in different trends.

CONCLUSIONS

The SPF rocks follow a tholeiitic trend, but they do not have the mid-ocean ridge characteristic of trace elements in chondritic ratios. Though Cummings and McCulloch (1992) characterize the SPF as a technically emplaced "sliver" of ocean crust, I would be cautious in comparing these highly altered Archean rocks to modern rock-types. In some ways these rocks are more analogous to Archean komatiitic basalts which exhibit LREE and Zr enrichment and non-chondritic Ti/Zr ratios (Cattell and Taylor, 1992) than any modern volcanic rock. Assigning a plate-tectonic provenance to these rocks is difficult until the plate-tectonic relationships of relatively unaltered Archean volcanics (such as greenstone belt successions) are better understood.

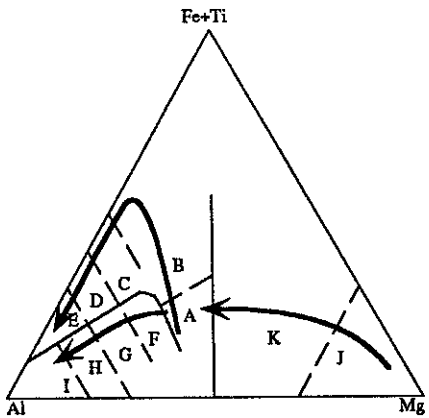

Figure 1. The Jensen Cation Plot (Jensen 1976) showing the **tholeiitic trend** (High-Magnesium Basalt (A)-> High-Iron Tholeiitic Basalt (B)-> Andesite (C)-> Dacite (D)-> Rhyolite (E)), the **calc-alkalic trend** (Basalt (F)-> Andesite (G)-> Dacite (H)-> Rhyolite (I)) and the **komatiitic trend** (Ultramafic Komatiite (J)-> Basaltic Komatiite (K)).

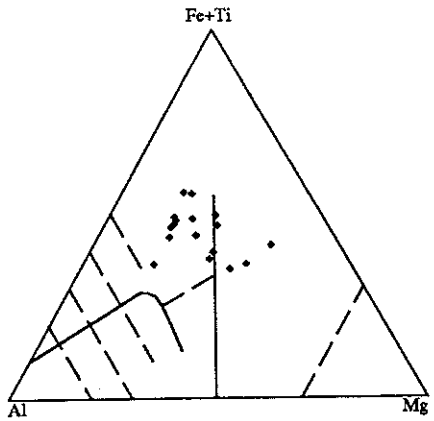

Figure 2. Jensen Cation plot (Jensen, 1976) of orthoamphibole-bearing rocks from the Spuhler Peak Formation (SPF).

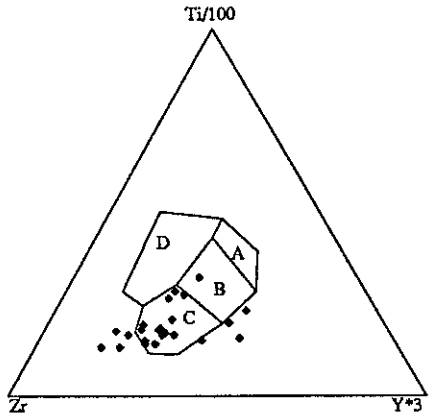

Figure 3. A plot of orthoamphibole-bearing SPF rocks on the Ti-Zr-Y discrimination diagram for basalts (Pearce and Cann, 1973). The fields are: A, island-arc tholeiites; B, MORB, island-arc tholeiites, and calc-alkali basalts; C, calc-alkali basalts; D, within-plate basalts.

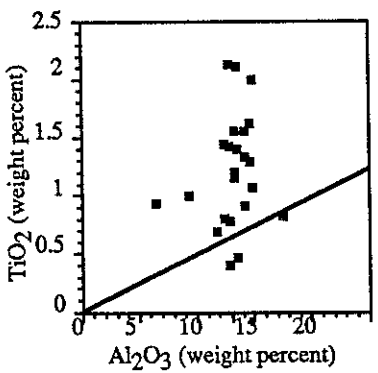

Figure 4. Plot of Al2O3 (weight percent) versus TiO2 (weight percent) for orthoamphibole-bearing SPF rocks. Reference lines are for chondrite (Sun, 1984).

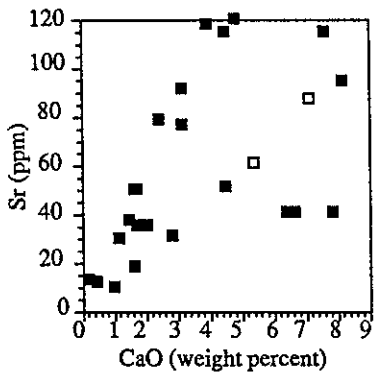

Figure 5. Plot of CaO (weight percent) versus Strontium (ppm) for Orthoamphibole-bearing rocks (filled) and non-orthoamphibole-bearing rocks (open) of the SPF. See text for discussion.

TABLE 1. Major elements (in oxide weight percents) and trace elements (in ppm). Locations are Spuhler Peak area (SP), Indian Ridge (IR), Mustard Pass area (MP), Gneiss Lake Area (GL), and Branham Lakes area (BL). * all iron as FeO.

Sample	1	2	3a	4	5	6b	7	11	12	13	14	15
SiO2	56.68	47.83	51.65	47.67	53.64	45.99	44.83	59.15	55.89	50.79	47.25	52.7
Al203	15.45	14.79	14.34	13.52	7.421	15.39	14.25	18.25	14.79	13.55	13.25	14.32
FeO*	8.72	12.84	14.68	15.96	12.38	17.15	17.71	9.205	10.75	16.17	12.93	14.92
MgO	5.258	9.597	8.5	12.77	17.41	11.18	12.85	5.86	5.884	6.187	18.72	8.673
CaO	8.258	1.708	2.235	1.886	1.883	1.519	1.698	.3458	4.095	6.739	1.149	2.622
Na2O	6.844	4.013	2.521	2.938	1.322	1.971	1.361	.4352	3.614	.8216	1.443	1.904
K2O	.4727	2.576	.476	.6653	.9902	1.395	.1364	2.894	.5242	.5611	.622	2.256
MnO	.1557	.1971	.3366	.0981	.1362	.1373	.2181	.2128	.2057	.2427	.1351	.1937
P2O5	.1173	.1402	.2884	.2729	.1252	.2352	.3787	.0649	.1981	.231	.124	.0934
TiO2	.9798	1.255	1.323	1.33	.8389	1.884	2.014	.725	.8254	2.035	.6964	.3847
Ba	74.07	493.4	32.54	121.4	85.81	229.6	33.94	463.4	155.4	146.5	23.05	252.6
Cr	106.1	139.2	94.01	21.01	705.3	83.4	47.39	368.4	115.5	189.2	611.7	2543
Be	1.041	1.061	1.309	1.742	.9689	.6042	.7367	.7099	2.398	1.874	1.429	1.026
Ce	27.6	30.73	57.23	74.3	39.44	37.47	95.32	33	44.49	33.09	37.11	17.89
Co	32.12	64.48	38.46	55.02	67.77	65.74	46.12	34.85	39.56	48.62	65.24	99.85
La	7.617	5.198	24.64	33.49	16.44	11.19	72.91	10.57	21.84	13613	16.14	6.214
Ni	73.4	147.2	21.51	20.86	724.7	101.3	25.41	155.7	61.59	90.88	167.8	775.9
Sc	29.94	33.19	43.33	32.83	19.24	33.99	69.3	20.17	34.73	41.87	37.27	39.42
Sr	74	49.81	33.42	47.39	33.89	36.55	17.58	12.17	117	41.04	8.776	76.58
V	202.6	294	279.6	337.1	131.4	269.4	293.2	149.9	209.9	394.1	208.8	182.2
Y	17.93	21.49	52.87	30.71	20.1	37.9	75.66	13.91	30	36.26	20.38	19.29
Yb	1.813	1.762	5.527	2.892	2.182	3.739	10.39	1.378	3.197	2.419	2.32	2.359
Zr	101	110.1	136.6	283	153.5	173.5	153.7	154.8	147.8	137.2	123	68.43
Area	IR	IR	IR	SP	SP	SP	SP	IR	IR	IR	IR	MP

Sample	16	17	18	20	21	26	27	29a	29b	29c	30
SiO2	48.93	63.1	54.73	55.82	51.07	50.19	49.06	48.87	53.23	54.93	50.4
Al203	13.64	10.16	15.14	12.5	13.97	13.78	13.7	14.08	15.12	14.83	13.32
FeO*	11.8	7.603	13.24	9.442	11.45	18.12	12.64	13.77	13.19	11.49	13.4
MgO	11.79	11.01	6.048	10.14	5.854	7.476	12.04	6.841	6.343	5.891	12.83
CaO	7.97	.6718	3.266	6.544	7.769	2.952	4.672	8.293	4.684	4.97	1.322
Na2O	1.701	1.194	3.081	2.377	3.549	2.185	2.866	2.641	4.493	3.769	2.155
K2O	1.35	.8442	.4488	.5264	.6762	.4791	1.035	.834	.4931	.6876	.5643
MnO	.262	.0376	.2357	.01334	.1955	.3951	.2516	.228	.1797	.1756	.1071
P2O5	.0732	.2395	.3665	.123	.3777	.1919	.0914	.1546	.1571	.4123	.3142
TiO2	.3289	.9145	1.557	.6108	1.46	1.113	.6856	1.073	1.215	1.467	1.376
Ba	115.5	21.01	49.82	39.12	287.7	54.96	62.96	124.7	81.88	125.1	25.46
Cr	1247	30.35	48.9	605.4	59.8	73.6	49.81	113.5	104.7	55.23	96.65
Be	1.159	1.213	2.209	1.246	2.463	1.021	1.238	2.195	1.506	2.668	2.233
Ce	29.73	36.96	72.59	25.41	76.73	36.48	10.75	23.32	27.5	50.83	40.31
Co	59.57	26.23	41.57	48.21	43.61	54.5	45.81	54.59	56.04	37.66	48.11
La	16.15	19.44	42.74	17.28	50.62	22.95	1.541	14.87	10.33	30.41	19.3
Ni	349.3	22.65	25.43	141.2	61.87	72.84	40.13	79.58	103.3	27.73	33.56
Sc	39.92	24.85	44.08	32.5	35.93	36.01	36.65	45.12	36.97	38.39	38.13
Sr	89.04	10.78	90.45	41.66	113.7	29.99	50.88	93.03	113	118.6	27.92
V	178.6	190.2	313	183.6	263.2	211.8	225.7	295.4	282.2	290.3	307.4
Y	19.54	34.17	50.66	20.09	50.25	35.04	18.26	30.47	27.44	43.55	30.56
Yb	2.42	3.873	5.543	2.48	5.485	3.727	1.827	3.142	2.482	4.328	3.004
Zr	45.31	206.4	289.2	109.6	344.4	244.3	93.38	177.4	208	425.5	415.6
Area	MP	MP	MP	IR	IR	SP	GL	BL	BL	BL	RL

REFERENCES CITED

Burger, H. R., 1966, Structure, petrology, and ecconomic geology of the Sheridan district, Madison County, Montana [Ph.D. thesis], Bloomington, Indiana, Indiana University, 156 p.

Cattell, A. C., and Taylor, R. N., 1992, Archaean basic magmas, *in* Hall, R. P. and Hughes, D. L., eds., Early Precambrian basic magmatism: Glasgow, Great Britain, Blackie, p. 12-39.

Cummings, M. L., and McCulloch, W. R., 1992, Geochemistry and origin of amphibolite and ultramafic rocks, Branham Lakes area, Tobacco Root Mountains, southwestern Montana, *in* Bartholomew, M. J., Hyndman, D. W., Mogk, D. W., and Mason, R. eds., Basment Tectonics 8: Characterization and comparison of ancient and Mesozoic continental margins - Proceedings of the 8th International Conference on Basement Tectonics (Butte, Montana, 1988): Dordrecht, The Netherlands, Kluwser Academic Publishers, p. 323-340.

Gillmeister, N. M., 1971, Petrology of Precambrian rocks in the central Tobacco Root Mountains, Madison County, Montana [Ph.D. thesis]: Cambridge, Massachusetts, Harvard University, 210 p.

Humphris, S. E., and Thompson, G., 1978a, Hydrothermal alteration of basalts by seawater: Geochimica et Cosmochimica Acta, v. 42, p. 107-125.

Humphris, S. E., and Thompson, G., 1978b, Trace element mobility during hydrothermal alteration of oceanic basalts: Geochimica et Cosmochimica Acta, v. 42, p. 127-136.

Irvine, T. N., and Baragar, W. R. A., 1971, A guide to the chemical classification of the common volcanic rocks: Canadian J. of Earth Sci., v. 8, p. 523-548.

Jensen, L. S., 1976, A new cation plot for classifying subalkalic volcanic rocks: Ontario Div. Mines, MP 66, 22p.

MacGeehan, P. J., and MacLean, 1980, An Archean sub-seafloor geothermal system, 'calc-alkali' trends, and massive sulfide genesis: Nature, v. 286, p. 767-771.

O'Neill, J. M., 1983, Geologic map of the Middle Mountain - Tobacco Root roadless area, Madison County, Montana: US Geological Survey Miscellaneous Field Studies Map MF-1590A.

Pearce, J. A., and Cann, J. R., 1973, Tectonic setting of basic volcanic rocks determined using trace element analyses: Earth Planet. Sci. Letters, v. 19, p. 290-300.

Reinhardt, J., 1987, Cordierite-anthophyllite rocks from north-west Queensland, Australia: metamorphosed magnesian pelites: Journal of Metamorphic Geology, v. 5, p. 451-472.

Robinson, P, Spear, F. S., Schumaker, J. C., Laird, J., Klein, C., Evans, B. W., and Doolan, B. L., 1982, Phase realtions in metamorphic amphiboles: natural occurence and theory, *in* Veblen, D. R., and Ribbe, P. H., eds., Amphiboles, minerology and experimental phase relations: Mineralogical Society of America, v. 9B, p. 1-211.

Sun, S. S., 1984, Geochemical Characteristics of Archaean Ultramific and Mafic Volcanic Rocks: Implications for mantle composition and evolution, *in* Kroner, A., Hanson, G. N., and Goodwin, A. M., eds., Archaean Geochemistry: Berlin, Germany, Springer-Verlag, p. 25-46.

Vitaliano, C. J., and Cordua, W. S., Comp., 1979, Geologic Map of the Southern Tobacco Root Mountains, Madison County, Montana: Geological Society of America Map and Chart Series MC-31, scale 1:62,500.

Origin, Metamorphic History, and Tectonic Setting of Archean Rocks from the Spuhler Peak Assemblage, Tobacco Root Mountains, MT

Chris Poulsen
Carleton College
Northfield, MN 55057

Introduction

The Spuhler Peak Assemblage's distinct lithologies stand out among the other lithological units of the Tobacco Root Mountains, located structurally above and below the Spuhler Peak Assemblage. Unlike the Indian Creek Metamorphic Suite (ICMS) and the Pony-Middle Mountain Metamorphic Suite (PMMMS) which are dominated by meta-sedimentary and meta-plutonic rocks, the Spuhler Peak Assemblage contains large quantities of amphibolite with smaller amounts of meta-sedimentary, meta-ultramafic, and other amphibole-rich rocks. These lithological differences between units of the Tobacco Root Mountains raise some interesting questions about the relationships between units. The goal of this project is to shed some light on the relationship between the Spuhler Peak Assemblage and the ICMS and PMMMS.

In this study, I examine the field relationships, petrology, and geochemistry of a suite of rocks exposed along Branham and Leggat Ridge, situated at the southeastern most portion of the Spuhler Peak Assemblage. My goal is to characterize the rocks in this suite, revealing their parent rocks, metamorphic history, and Archean tectonic setting. Additionally, I focus on the ultramafic rocks found throughout the Spuhler Peak Formation. These rocks have received little attention, but are potentially very important for understanding the tectonics of the region.

Field Relationships

Both Branham Ridge and Leggat Ridge contain good exposures of Spuhler Peak lithologies. They trend northeast-southwest, though a small portion of Leggat Ridge trends nearly east-west. Foliations along the ridges are fairly constant, striking to the northwest and dipping moderately to steeply (45-85°) to the northeast. The only significant deviation is caused by an isoclinal fold on Leggat Ridge.

The Spuhler Peak Assemblage, as exposed on Leggat and Branham ridges, includes interlayered amphibolite, hornblende-plagioclase-quartz gneiss, other amphibole-rich rocks, quartzite, sillimanite-bearing quartz-plagioclase-garnet-biotite schist. Lithologies vary greatly in thickness (<1m to more than 300m) and are commonly discontinuous or covered by talus, making mapping of individual lithologies nearly impossible. In order to determine relationships between the lithologies, I measured their thicknesses perpendicular to the foliation along the Spuhler Peak and Branham ridges. (See figures 1 and 2.)

In contrast to the interlayered lithologies, the meta-ultramafic rocks occur as layers and pods with thicknesses from 10 to 20 meters and lengths from 10 to a few hundred meters. The longer meta-ultramafic bodies are conformable to compositional layering in the amphibolite (Cummings and McCulloch, 1989). The meta-ultramafics are separated from adjacent amphibolite by a reaction rim of black hornblende gneiss. However, at two exposures (one within my field area and one on Spuhler Peak Ridge) the contact is zoned and includes hornblende, actinolite, biotite, and chlorite-rich layers.

The other amphibole-rich rocks are found in a variety of relationships. On Branham Ridge, they occur as a massive, discontinuous unit. They are also found adjacent to amphibolite and pelitic rocks on Leggat Ridge and in the valley separating Leggat Ridge from Branham Ridge. In these occurrences, there is no sharp contact between lithologies. The amphibolite and pelitic rocks grade into the other amphibole-rich lithologies which are less than a meter thick.

Petrography

Amphibolites. Amphibolite may be a misnomer, since the rocks in this category are not always dominated by hornblende and plagioclase. These rocks are dark colored and show either a salt and pepper texture or leucocratic stringers of quartz and plagioclase, in which case they are probably better referred to as hornblende-plagioclase-quartz gneiss. Hornblende is the main component of these rocks, varying in concentration from 30 to 70%, and plagioclase is an important component, making up 5-40% of the bulk composition. Quartz and garnet are abundant in the hornblende-plagioclase-quartz gneiss, varying between 5 to 40% and 0 to 24%, respectively. Minor minerals include opaques, epidote, chlorite, talc, actinolite, apatite, zircon, biotite, and spinel. Some of these rocks have a weak foliation with garnets commonly exhibiting fractures perpendicular to foliation.

Quartzites and Quartzofeldspathic schist . Siliclastic metamorphic rocks range in composition from a nearly pure quartzite (93% quartz) to a sillimanite-bearing, plagioclase-quartz-garnet-biotite gneiss. These rocks are dominated by quartz (30-93%), plagioclase (0-40%), biotite (1-50%), and garnet (0-40%). Minor components include sillimanite (1-10%), chlorite (<1%), muscovite (<1-3%), opaques (<1%), phlogopite (1%), and zircon (<1%). Two forms of sillimanite are present, a slender prismatic form and a fibrolitic form. The slender prismatic form of sillimanite is uncommon and probably originated at higher pressures and temperatures than the fibrolite form (Yardley, 1989). Pelites exhibit a strong foliation and are compositionally banded into quartzofeldspathic layers and biotite-garnet-sillimanite layers with smaller amounts of quartz and plagioclase.

Meta-ultramafics. The meta-ultramafic rocks are dark green and gray rocks, and vary from fine-grained to very coarse-grained. The meta-ultramafics differ considerably in the amount of metamorphic alteration they have undergone, with one sample composed of 70% talc and other samples devoid of talc. Relict olivine and relict orthopyroxene (up to 1 cm) are present in all of the samples, though usually not together in the same sample. Tremolite-actinolite replaces the olivine and orthopyroxene. Other minerals common in the meta-ultramafics are chlorite, opaques, and rutile. Foliation is poorly developed, although chlorite usually shows a preferred orientation.

Hornblende gneiss. As mentioned above, these rocks surround the meta-ultramafics at their contact with the amphibolites. They are easily recognizable by their black color and coarse grain size (up to 8-9 cm). Hornblende (97-98%) is the principal mineral, but minor amounts of plagioclase, quartz, chlorite, opaques, epidote, garnet, and apatite are present.